Effect of Solution Concentration on the Properties of Nanocomposites

Madhuchhanda Maiti, Anil K. Bhowmick

Rubber Technology Centre, Indian Institute of Technology, Kharagpur-721302, India

Received 8 June 2005; accepted 31 October 2005
DOI 10.1002/app.23885
Published online in Wiley InterScience (www.interscience.wiley.com).

ABSTRACT: Though a large number of nanocomposites prepared by solution process has been reported in the literature, effect of solution concentration on properties of the nanocomposites has not been studied. In the present work, new fluorocarbon–clay nanocomposites were prepared by a solution mixing process. Characterization of the nanocomposites was done with X-ray diffraction technique and atomic force microscopy. Effects of different rubber-solution concentrations (5, 10, 15, 20, and 25 wt %) on the mechanical and dynamic mechanical properties of the resultant nanocomposites were investigated. Optimum properties were achieved at 20 wt % solution. The data could be explained with the help of structure of the nanocomposites and dispersion of the clay. © 2006 Wiley Periodicals, Inc. J Appl Polym Sci 101: 2407–2411, 2006

Key words: nanocomposites; fluoroelastomer; clay; X-ray diffraction; atomic force microscopy

INTRODUCTION

Polymer–clay nanocomposites continue to be an area of great interest due to dramatic improvements in properties that these materials have over conventional composites.[1,2] These show better thermal, mechanical, barrier, and other properties because of excellent dispersion of filler and stronger interfacial force between the well dispersed nanometer-sized domains and a polymer, than the conventional polymer/filler composites.[3–10] Depending on the structure of clay particles in a polymer matrix, nanocomposites can be classified as either intercalated or exfoliated.

Polymer nanocomposites can be prepared mainly by three techniques—*in-situ* polymerization, solution mixing, and melt mixing.[1–10] Though melt mixing is industrially more acceptable, solution mixing provides better improvements in properties.[11,12] It has been also observed that dispersion of clay is always superior in solution mixing to melt mixing. If the solution concentration is optimized by using minimum solvent, yet providing best properties, this may reduce the cost of production and will be very helpful from the industrial point of view. Though there is large number of studies, where nanocomposites have been prepared by solution process, the earlier authors have not reported the concentration of the polymer-solutions.[13–20] Detailed mixing procedures have also not been disclosed in many of the investigations, although these are very important in deciding the magnitude of properties. However, measurement of morphology, permeability, flammability, mechanical properties, etc. has been done on these nanocomposites. While an attempt is made to compare properties of different nanocomposites reported by several authors, it is found that the conditions like nature of solvent, temperature, clay loading etc. are different in these investigations, which do not allow us for a real comparison. However, a literature search shows that there is 10–300% change in tensile modulus depending on the polymer matrix at 3–5 wt % of sodium montmorillonite or organoclay loading.[7,9,13–20] Hence, there is no article available on the study of the effect of solution concentration on the properties of nanocomposites. Literature survey also shows that extensive research work has been done on nanocomposites based on many general purpose polymers including different plastics, rubbers, and thermoplastic elastomers.[1–28] However, there is very little work done on specialty rubbers such as fluoroelastomer, which has space application where lighter weight but stronger material is required.[29]

This article highlights the preparation and the properties of the fluoroelastomer–sodium montmorillonite clay nanocomposites at different solution concentrations.

EXPERIMENTAL

Materials used

Viton B-50 [a terpolymer of vinylidene fluoride, hexafluoropropylene and tetrafluoroethylene, density

Correspondence to: A. K. Bhowmick (anilkb@rtc.iitkgp.ernet.in).

1850 kg/m^3 at 25°C, 68% F] was procured from DuPont Dow Elastomers, Freeport, TX. Nanoclay, Cloisite NA+ was obtained from Southern Clay Products, Gonzales, TX. Methyl ethyl ketone was supplied by Nice Chemicals, Cochin, India.

Sample preparation

The rubber was first dissolved in methyl ethyl ketone to make 5, 10, 15, 20, and 25 wt % solutions. Four parts per hundred gram of rubber (4 phr, i.e., filler weight fraction of 3.85% or volume fraction of 2.52%) of sodium montmorillonite clay was dispersed in methyl ethyl ketone. The concentration of the nanofiller was selected from the knowledge of our earlier work.[9] Then, it was added to the rubber solution and thoroughly stirred at 2000 rpm for 3 h at room temperature in a mechanical stirrer (Remi Motors, Mumbai, India) to make a homogeneous mixture, which was then cast and kept in air, followed by vacuum treatment for 24 h to drive off the solvent.

Samples are designated as FWXC4 where F stands for fluoroelastomer, WX indicates the solution concentration and C4 indicates four parts of clay loading.

Characterization

X-ray diffraction studies (XRD)

For the characterization of the rubber nanocomposites, XRD studies were performed using a PHILIPS X-PERT PRO diffractometer in the range of 2°–9° (2θ) and Cu-target ($\lambda = 0.154$ nm). Then, d-spacing of the clay particles was calculated using the Bragg's law. The samples were placed vertically in front of the X-ray source. The detector was moving at an angle of 2θ while the sample was moving at an angle of θ.

Atomic force microscopy (AFM)

Multi Mode Scanning Probe Microscope model with a Nanoscope IIIa controller by Digital Instruments Inc. (Veeco Metrology Group), Santa Barbara, CA was used for the atomic force microscopy (AFM) studies. The AFM measurements were carried out in air at ambient conditions (25°C) using tapping mode probes with constant amplitude (40 mV). The rotated tapping mode etched silicone probe (RTESP) [square pyramid in shape with a spring constant of 20 N/m, nominal radius of curvature of 10 nm] with resonance frequency of 270 kHz was used. Height and phase images were recorded simultaneously at the resonance frequency of the cantilever with a scan rate of 1 Hz and a resolution of 256 samples per line. This allowed the resolution of individual primary particle measurements. The images were analyzed using a nanoscope image processing software (5.30r1).

Brookfield viscosity

Viscosity of the solutions was measured using a R/S Brookfield rheometer (DIN 53109 and DIN 53453 with rotating spindle/stationary chamber) in a programmed shear rate mode at 25°C.

Mechanical properties

Tensile specimens were punched out from the cast sheets using ASTM Die - C. The tests were carried out as per the ASTM D 412–98 method in a Universal Testing Machine (Zwick 1445) at a cross-head speed of 500 mm/min at 25°C. The average of three tests is reported here.

Dynamic mechanical thermal analysis

The dynamic mechanical spectra of the nanocomposites were obtained by using a DMTA IV, (Rheometric Scientific, NJ) dynamic mechanical thermal analyzer. The sample specimens were analyzed in tensile mode at a constant frequency of 1 Hz, a strain of 0.01% and a temperature range from –50 to 80°C at a heating rate of 2°C/min. The data were analyzed by RSI Orchestrator application software on an ACER computer attached to the machine. Storage modulus (E'), loss modulus (E''), and loss tangent (tan δ) were measured as a function of temperature for all the samples under identical conditions. The temperature corresponding to the peak in loss modulus versus temperature plot

TABLE I
Mechanical Properties of Different Composites

Sample name	Solution concentration (wt %)	Brookfield Viscosity (10^2 Pa s)	Modulus at 100% elongation (MPa)	Elongation at break (%)	Maximum stress (MPa)
F	20	0. 6	0.35 ± 0.08	110 ± 5	0.46 ± 0.02
FW5C4	5	0.1	0.66 ± 0.04	120 ± 5	0.70 ± 0.05
FW10C4	10	0.6	0.80 ± 0.01	350 ± 10	0.90 ± 0.01
FW15C4	15	1.5	0.82 ± 0.01	390 ± 10	0.90 ± 0.01
FW20C4	20	49.0	0.88 ± 0.01	520 ± 5	0.90 ± 0.01
FW25C4	25	53.9	0.79 ± 0.01	590 ± 10	0.80 ± 0.01

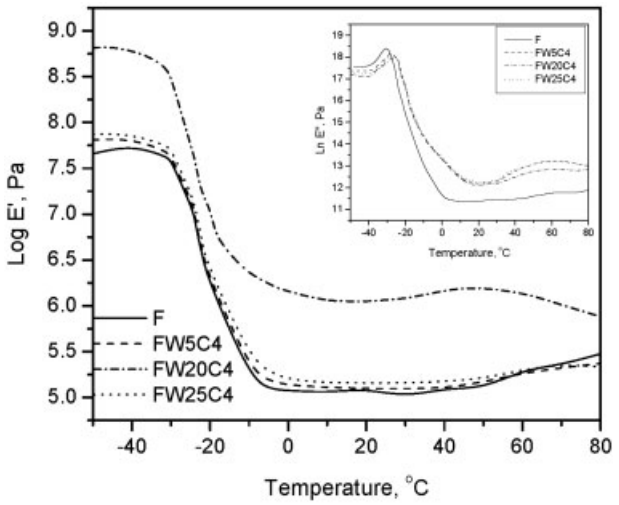

Figure 1 Plot of storage modulus versus temperature; Inset: Plot of loss modulus versus temperature.

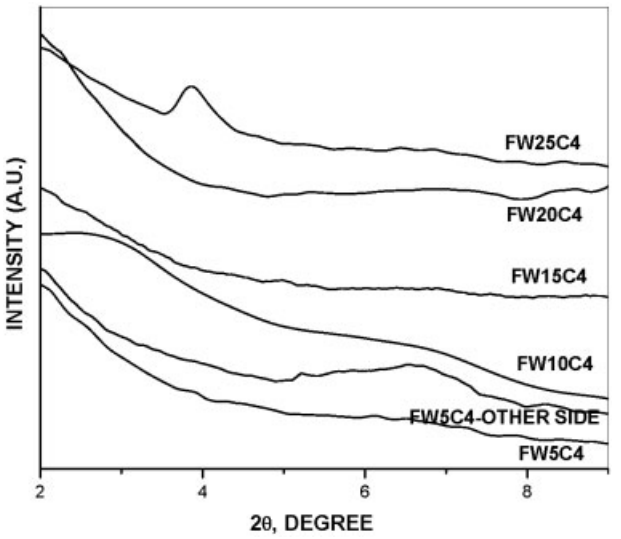

Figure 2 XRD of nanocomposites prepared at different solution concentrations.

was taken as the glass-rubber transition temperature (T_g).

RESULTS AND DISCUSSION

To study the effect of solution concentration on the mechanical properties, rubber–clay composites were prepared at five different rubber-solution concentrations keeping the clay loading same (filler weight fraction of 3.85%). Their mechanical properties are listed in Table I.

While the neat polymer films cast from different concentrations exhibit same strength (0.46 ± 0.02 MPa), the strength of the nanocomposites is a function of the solution concentration.

The composites FW5C4, FW10C4, FW15C4, FW20C4, and FW25C4 show 89, 129, 134, 151, and 126% improvement in tensile modulus, 52, 96, 96, 96, and 74% increment in maximum stress, and 10, 220, 250, 370, and 440% increase in elongation at break, respectively over the neat fluorocarbon rubber. Hence, the 20 wt % solution exhibits highest tensile modulus (0.88 ± 0.01 MPa) and maximum stress (0.90 ± 0.01 MPa) of the resultant solid nanocomposite, while 25 wt % solution gives maximum elongation at break [(590 ± 10)%].

Figure 1 illustrates the storage modulus versus temperature curves with loss modulus versus temperature curves as inset for F, FW5C4, FW20C4, and FW25C4. For sake of clarity, the results of only four samples are given in the figure. Storage modulus increases with the addition of the clay compared to the neat polymer upto 60°C. FW20C4 exhibits the highest storage modulus followed by FW15C4, FW10C4, FW25C4, and FW5C4, over the whole temperature region. The dynamic mechanical properties at selected temperatures are reported in Table II. The storage modulus of the nanocomposite film at 25°C is increased by 19%, while the concentration is changed from 5 to 20 wt %. It is clear that the modulus increases gradually upto 20 wt %. The modulus decreases after 20 wt % concentration. The T_g shift, calculated from the loss modulus curves shown in the inset, is also highest in the case of FW20C4, exhibiting best polymer–filler interaction. The peak maxima of the film is also reduced at 20 wt % concentration (Fig. 1).

The Brookfield viscosity value, however, has an increasing trend as the concentration of the solution is increased (Table I). There is an abrupt change at 20 wt %. This may be due to the fact that an equilibrium adsorption of the rubber chains on the clay particles is possible at this concentration, which leads to the transient network or gel formation, and the diffused rubber chains further serve as a bridge between neighboring clay particles.[30] So, at this concentration, a better interfacial adhesion between the clay particles and the polymer matrix has been established. This physical gel formation and the interactions between polymer–filler greatly affect the viscoelastic properties.[31] Thus poly-

TABLE II
Dynamic Mechanical Properties of Different Composites

Sample name	T_g (°C, from loss modulus)	log E'' at T_g (Pa)	log E' at 25°C (Pa)
F	−30	8.12	5.06
FW5C4	−28	7.95	5.09
FW10C4	−27	7.93	5.97
FW15C4	−27	7.86	6.00
FW20C4	−26	7.82	6.04
FW25C4	−28	7.90	5.18

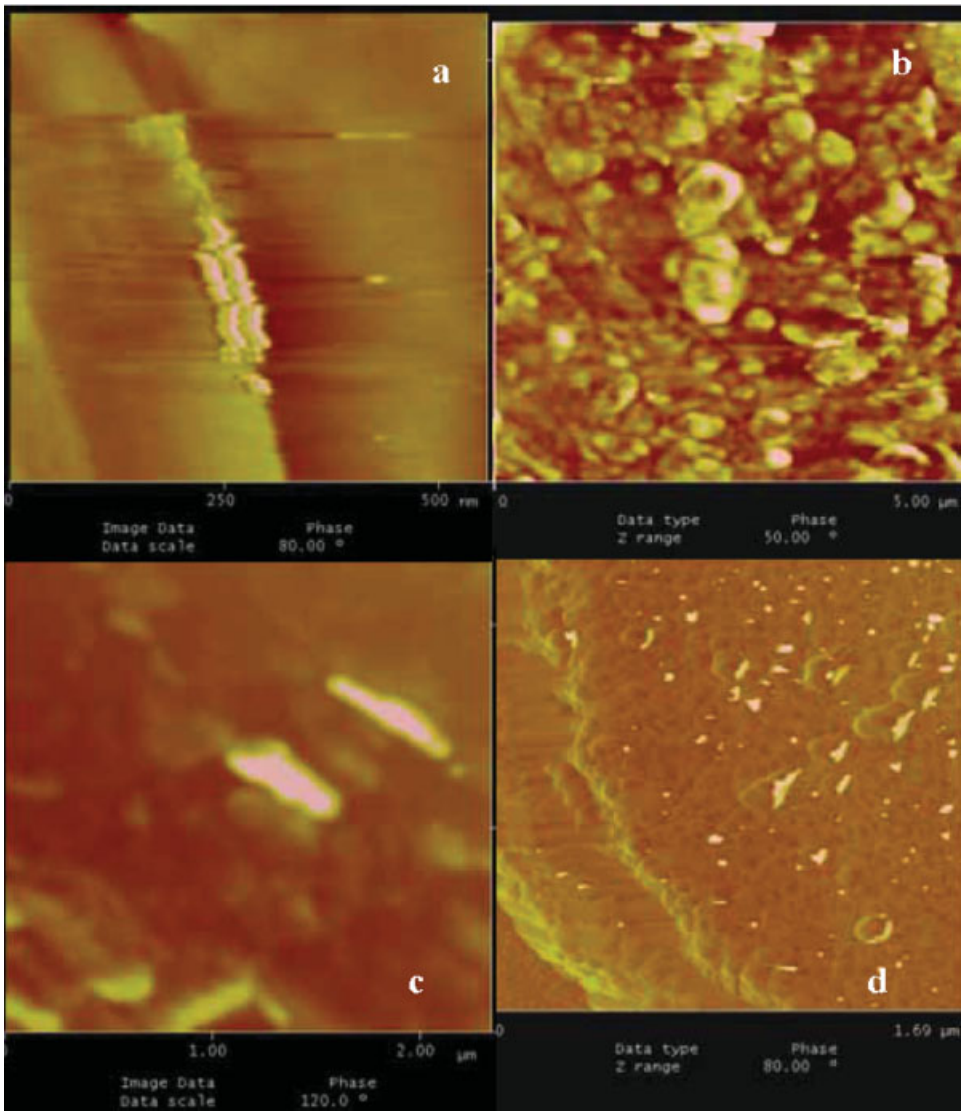

Figure 3 AFM micrographs of (a) FW5C4 (top surface), (b) FW5C4 (lower surface), (c) FW25C4, and (d) FW20C4. [Color figure can be viewed in the online issue, which is available at www.interscience.wiley.com.]

mer–filler interaction increases at this concentration, which may also be the reason for the change in the mechanical and dynamic mechanical properties at this concentration. However, these results are best understood from the morphological analysis.

X-ray diffractograms of the composites, shown in Figure 2, reveal that there is no peak in the region of 2°–9° (2θ) for solution concentration upto 20 wt %. At higher concentration (25 wt %), a small peak at 3.9° appears. The neat clay, Cloisite NA+, shows a peak at 7.5°.[32] Hence, absence of any peak upto 20 wt % concentration, simply indicates that the clays are exfoliated up to this concentration. Beyond this concentration, rubber chains intercalate in the clay galleries, as there is a peak shift towards lower 2θ value in the case of 25 wt % concentration. AFM results, as discussed later, also corroborate this observation.

However, at very low concentration (5 wt %), poor mechanical properties are observed in spite of exfoliation of the clays. At this concentration, decoiling of the polymer chains takes place and the chains are individually solvated resulting in an increase in hydrodynamic volume. In such a condition, polymer–solvent interaction dominates over the polymer–filler interaction. As the polar solvent is present in higher amount, the clays are swelled and the surface area of clay in such a dispersion grows dramatically. However, the chances of interaction between the matrix and the clay are low due to high dilution. As a result, there is a possibility of clay particles settling down during the preparation of the film. The AFM micrograph shows very few particles on the top surface [Fig. 3(a)]. The particles present on the top surface are 10–12 nm wide. Hence, XRD does not show any peak.

Most of the clay particles having dimension of 60 to 80 nm are precipitated on the other surface of the cast film [Fig. 3(b)]. The X-ray diffractogram of this surface shows a broad hump in between 6 ° and 7°, which corroborates that there are some agglomerations of the clays on this side (Fig. 2).

At high concentration (25 wt %), deterioration of both the mechanical and the dynamic mechanical properties can be explained with the XRD diagram shown in Figure 2. There is a peak at 3.9° (2θ), indicating intercalation of the clays. At higher concentration, as the polymer to solvent ratio increases, polymer–polymer interaction is much prominent than polymer–solvent or polymer–filler interaction. Hence, decoiling of polymer chains does not take place extensively. So, the coiled polymer chains cannot diffuse into the gallery-gaps of the clay so easily. In other words, it can be said, exfoliation of the clays is inhibited at higher concentration. The AFM [Fig. 3(c)] photograph also supports this phenomenon by showing that the clay particles are agglomerated in some places (having an average particle width of ~80 nm) and are not homogeneously distributed.

Tensile properties optimize at 20 wt % solution. The storage modulus of the resultant film is also highest at this solution concentration only (Fig. 1). Beyond this critical solution concentration, the properties deteriorate. The enhanced properties at this 20 wt % concentration may be due to the better polymer–filler interaction as evident from the XRD (Fig. 2) and better clay dispersion shown by AFM [Fig. 3(d)]. There are mainly three types of interactions possible—polymer–polymer, polymer–solvent, and polymer–filler. Here, the last one is favored over the other two types of interactions. The XRD diagram shows exfoliation, as there is no peak. The AFM micrograph also shows exfoliation with an average particle width of 8–10 nm. It also illustrates uniform distribution of clay particles in the matrix. Hence, it forms true nanocomposites at this concentration.

CONCLUSIONS

In solution mixing process, formation of nanocomposites and their mechanical and dynamic mechanical properties are a function of the concentration of rubber-solution at a constant filler loading, keeping all other processing parameters constant. These are found to be optimized at 20 wt % rubber-solution for fluoroelastomer–methyl ethyl ketone–sodium montmorillonite system. Both at the lower and higher concentrations, the properties are lower. The results are explained with the help of XRD and AFM.

References

1. Kojima, Y.; Usuki, A.; Kawasumi, M.; Fukushima, Y; Okada, A.; Kurauchi, T.; Kamigaito, O. J Mater Res 1993, 8, 1185.
2. Kojima, Y.; Usuki, A.; Kawasumi, M.; Okada, A.; Kurauchi, T.; Kamigaito, O. J Polym Sci Part A: Polym Chem 1993, 31, 983.
3. Chen, G.; Liu, S.; Chen, S.; Qi, Z. Macromol Chem Phys 2001, 202, 1189.
4. Li, X.; Kang, T. K.; Cho, W. J.; Lee, J. K.; Ha, C. S. Macromol Rapid Commun 2001, 22, 1306.
5. Messermith, P. B.; Giannelis, E. P. Chem Mater 1994, 6, 1719.
6. Burnside, S. D.; Giannelis, E. P. Chem Mater 1995, 7, 1597.
7. Sadhu, S.; Bhowmick, A. K. J Polym Sci Part B: Polym Phys 2004, 42, 1573.
8. Cho, J. W.; Paul, D. R. Polymer 2001, 42, 1083.
9. Maiti, M.; Sadhu, S.; Bhowmick, A. K. J Polym Sci Part B: Polym Phys 2004, 42, 4489.
10. Lan, T.; Pinnavaia, T. J. Chem Mater 1999, 6, 2216.
11. Shen, Z.; Simon, G. P.; Cheng, Y. B. Polymer 2002, 43, 4251.
12. Liang, Y; Wang, Y; Wu, Y; Lu, Y; Zhang, H; Zhang, L. Polym Test 2004, 24, 12.
13. Strawhecker, K. E.; Manias, E. Chem Mater 2000, 12, 2943.
14. Lim, S. T.; Hyun, Y. H.; Choi, H. J.; Jhon, M. S. Chem Mater 2002, 14, 1839.
15. Lim, S. K.; Kim, J. W.; Chin, I.; Kwon, Y. K.; Choi, H. J. Chem Mater 2002, 14, 1989.
16. Plummer, C. J. G.; Garamszegi, L.; Leterrier, Y.; Rodlert, M.; Manson, J. E. Chem Mater 2002, 14, 486.
17. Sur, G. S.; Sun, H. L.; Lyu, S. G.; Mark, J. E. Polymer 2001, 42, 9783.
18. Pramanik, M.; Srivastava, S. K.; Samantaray, B. K.; Bhowmick, A. K. J Polym Sci Part B: Polym Phys 2002, 40, 2065.
19. Chen, B.; Evans, J. R. G. Polym Int 2005, 54, 807.
20. Malwitz, M. M.; Lin-gibson, S.; Hobbie, E. K.; Butler, P. D.; Schmidt, G. J Polym Sci Part B: Polym Phys 2003, 41, 3237.
21. Alexandre, M.; Dubois, P. Mater Sci Eng 2000, 28, 1.
22. Kornmann, X.; Lindberg, H.; Berglund, L. A. Polymer 2001, 42, 4493.
23. Pattanayak, A.; Jana, S. C. Polymer 2005, 46, 5183.
24. LeBaron, P. C.; Wang, Z.; Pinnavaia, T. J. Appl Clay Sci 1999, 15, 11.
25. Ray, S. S.; Okamoto, M. Prog Polym Sci 2003, 28, 1539.
26. Vergese S, Karger-Kocsis, J. Polymer 2003, 44, 4921.
27. Sadhu, S.; Bhowmick, A. K.; Rubber Chem Technol 2003, 76, 860.
28. Choi, M. H.; Chung, I. Z.; Lee, Z. D. Chem Mater 2000, 12, 2977.
29. www.dupont-dow.com/viton, accessed on 24 September 2004.
30. Swenson, J; Smalley, M. V.; Hatharasinghe, H. L. M.; Fragneto, G. Langmuir 2001, 17, 3813.
31. Lin-Gibson, S.; Kim, H.; Schmidt, G.; Han, C. C.; Hobbie, E. K. J Colloid Interface Sci 2004, 274, 515.
32. Maiti, M.; Bhowmick, A. K. J Polym Sci Part B: Polym Phys 2006, 44, 162.